Pervaporation performance of crosslinked PVA membranes in the vicinity of the glass transition temperature

Liang Liu, Sandra E. Kentish*

Department of Chemical Engineering, School of Chemical and Biomedical Engineering, The University of Melbourne, Vic. 3010, Australia

*Corresponding author.

E-mail address: sandraek@unimelb.edu.au

Abstract

This work investigates the pervaporation performance of crosslinked poly (vinyl alcohol) PVA membranes for ethanol dehydration near the glass transition. The solubility of water and ethanol mixture in the membranes was measured as a function of feed composition and sorption temperature, and the data was modelled by perturbed-chain statistical associating fluid theory (PC-SAFT). Importantly, this approach allows the solubility of the two components to be determined individually. Model results show that the heat of sorption of water and ethanol was constant across the temperature range. Water permeance generally decreased when operational temperature increased, indicating a solubility-controlled transport behavior. The permeance also increased when water feed concentration increased. Activation energy analysis provided more insights about the influence of membrane properties on the mass transport mechanism. At 90 wt% ethanol feed composition, the apparent activation energy (E_a) for water permeation changed from 9.6 kJ mol^{-1} when temperature was <70 °C to -9.1 kJ mol^{-1} when temperature was >80 °C. When the feed composition decreased to 80 wt% ethanol, a transition was observed at a lower temperature range (60-65 °C). These changes were related to changes in the activation energy of diffusion, given the heat of sorption was constant. The permeability of ethanol was lower due to its larger molecular size, but a similar transition was observed for the 80 wt% ethanol case.

Keywords: Poly (vinyl alcohol); mixture sorption; PC-SAFT; glass transition.

Introduction

Pervaporation (PV) is a novel membrane separation technology with high efficiency and energy saving benefits for liquid mixture separation, in particular, for azeotropic mixtures [1–3]. The membrane contacts with the liquid mixture on the feed side, while permeate is removed as a vapour [4]. The mass transport is driven by the vapour pressure difference between the feed solution and the permeate vapour. The solution-diffusion model is applicable for the transport of penetrants through such a membrane [5]. One component in the feed solution can be preferentially removed due to its higher affinity with the membrane polymer and/or higher diffusivity in the membrane. PV membranes have been developed for different applications including dehydration of organic solvents [6–8], removal of volatile organic compounds from water [9] and organic-organic separation [10]. Among these applications, dehydration of organic solvents is best developed. The solubility of water is high due to the use of a hydrophilic polymer and the diffusivity of water is also high because of its small molecular size compared with organic solvents. Hence, a high water selectivity can be achieved.

Many hydrophilic polymers have been investigated as pervaporation membranes for organic solvent dehydration [11,12]. Poly (vinyl alcohol) (PVA) is one of the most well-known as it has high hydrophilicity, is easy to process and is readily available [2]. However, pristine PVA is not suitable for membrane applications because it is can dissolve in aqueous solutions. Various cross-linkers have been used to improve the performance of PVA-based pervaporation membranes, such as glutaraldehyde [13–15], citric acid and maleic acid [16]. Another strategy to improve membrane performance is to develop a mixed matrix membrane (MMM), where an inorganic phase is introduced into the polymer matrix [3].

Although much experimental work have been reported in the literature for pervaporation [16], there is limited theoretical modeling work due to the complexity of the water-organic solvent mixture, which has significant non-ideality. Sorption isotherms can be convex (Type I isotherm) often described empirically by the dual mode sorption model; an S-shape (Type II isotherm) often described using the Guggenheim-Anderson-de Boer (GAB) model; or concave (Type III isotherm) [17].

Lue et al.[18] reported that the UNIQAC-HB (UNIversal QUAsi Chemical model accounting for the hydrogen bonding effect) could provide a model for mixed ethanol/water sorption in PDMS at 298 K. The Perturbed-Chain Statistical Associating Fluid Theory (PC-SAFT) equation of state is an advanced model that can model polymer systems [19–21] and might provide a better approach for modeling sorption of such organic liquid/water mixtures. It provided excellent results for the sorption of five different volatile organic carbons (VOCs) in two glassy polymers (i.e. Matrimid 5218 and P84) [22].

The transport behavior of penetrants in pervaporation membranes is generally analyzed as a function of temperature and/or feed concentration, and activation energy (E_a) is widely used [16,23,24]. A wide range of E_a from positive to negative has been reported [24]. Nevertheless, a single value of E_a is usually reported within the operational temperature range. However in other work, this activation energy has been observed to change. We found the activation energy of water changed from a positive value at 30 to 50 °C to an negative value at 50-150 °C for a Sulphonated Poly(Ether Ether) Ketone (SPEEK) [25]. This change could not be related to a simple glassy to rubbery transition. Rather we speculated that the falling diffusion coefficient with increasing temperature related to 'antiplasticisation'. This is a well known phenomenon caused by a loss of free volume in the polymer, as the penetrant accumulates in the larger voids. The Wessling group reported similar results [26], but in a later paper argued that such changes related to relaxation phenomena rather than antiplasticisation [27]. Similarly, Sato et al.[28] studied the behavior of a range of polymers exposed to benzene and water vapor and showed that water tended to cause antiplasticisation in polymers that were rubbery or close to the glass transition temperature, but plasticization occurred for water vapor when the polymer was fully glassy.

In this work, crosslinked PVA membranes for ethanol dehydration were prepared using glutaraldehyde as a cross-linker. First of all, the liquid sorption capacity of the membrane was studied at various solution compositions including pure ethanol, 90 wt%, 85 wt%, 80 wt%, 75 wt% ethanol concentration and pure water from 45 to 90 °C. Then the sorption data was modelled and analyzed using the PC-SAFT model. The influence of both operational temperature (45-90 °C) and feed composition (80, 85 and 95 wt%) on the pervaporation performance was investigated. Finally, the transport behavior of both water and ethanol was evaluated by analyzed the permeance, apparent activation energy and sorption and diffusion selectivity of both components in the PVA membrane.

Experimental

Poly (vinyl alcohol) (average molecular weight: 89000-98000, 99+% hydrolyzed) was purchased from Sigma Aldrich and was used without purification. 25 wt% glutaraldehyde aqueous solution was provided by Merck. Hydrochloric acid of 32 wt% was purchased from Ajax Finechem. Ultrapure water was produced using Millpore Elix®20.

A 10 wt% PVA aqueous solution was prepared at 90 °C under vigorously stirring and then was cooled down to room temperature. Hydrochloric acid and glutaraldehyde was then introduced at a molar crosslinking ratio of glutaraldehyde to vinyl alcohol monomer of 0.05. The molar ratio of hydrochloric acid to vinyl alcohol monomer was 0.05. PVA membranes were then fabricated by casting the solution onto a glass plate using a casting knife of 400 μm thickness, and were dried at room temperature overnight. They were then dried at 60 °C for 4 hours then annealed at 130 °C for 1.5 hours under vacuum. The membrane thickness was measured using a micrometer and was in the range of 40-60 μm with a variation less than 5 μm for each membrane All membranes were kept in a vacuum desiccator before use.

All membranes were dried under vacuum for 24 hours before liquid sorption measurement. Then the membranes were weighed using a digital microbalance and immersed in pure water, 75 wt% (ethanol concentration), 80 wt%, 85 wt%, 90 wt% and pure ethanol solutions in sealed bottles at temperatures from 45 to 90 °C. After 24 hours, the membranes were wiped clean with a tissue and then again weighed as quickly as possible. This process was repeated 2-3 times until sorption equilibrium was reached. Each liquid sorption measurement was repeated twice.

In a separate sequence of sorption experiments, some very thick membranes (500-600 μm) were prepared to increase the total mass of sorbed penetrant. Ethanol and water solutions were absorbed as above at 45 °C. The composition of the sorbed mixture in the membrane at 75 wt%, 80 wt% and 85 wt% was then determined by desorption at ambient temperature into a cold trap under vacuum for five hours. The water/ethanol mixture collected in the cold trap was analyzed by a Varian 7890B gas chromatograph (GC) with an Agilent HP-5 column (30 m*0.32 mm*0.25 μm) and a flame ionization detector (FID).

The sorption data was analyzed using the PC-SAFT equation of state [19,29,30]. This model is based on perturbation theories, where the total interaction of molecules is described by a reference fluid in which no attractive interactions occur, but which is perturbed by attractive interactions. The PC-SAFT model uses a hard-chain fluid as the reference fluid. The attractive interactions can be separated into dispersive interactions, association interactions and other interactions depending on specific systems [31]. The general expression of the model is shown in Eq. 1, where the residual Helmholtz free energy (A^{res}) is consisted of a hard chain contribution (A^{hc}), a dispersion contribution (A^{disp}) and an association contribution (A^{assoc}).

$$A^{res} = A^{hc} + A^{disp} + A^{assoc} \quad (1)$$

For a non-associating component, only the hard-chain term and the dispersion term is used to model its thermodynamic properties and only three pure-component parameters are needed: the segment diameter (σ_i), the segment number (m_i) and the dispersion energy parameter (??$/k$). For associating components (e.g. water and ethanol), the association term is added and two additional parameters (i.e. the association energy ($\varepsilon^{A_iB_i}$) and the association volume ($k^{A_iB_i}$)) are used. The number of association sites (N^{ass}) can be determined by consideration of the chemical structures. Table 1 shows the pure component PC-SAFT parameters for PVA, ethanol and H_2O.

Table 1: pure-component PC-SAFT parameters

	M (g/mol)	m^{seg}/M^a (mol/g)	σ (Å)	ε/k (K)	N^{ass} (-)	$k^{A_iB_i}$ (-)	$\varepsilon^{A_iB_i}/k$ (K)	Ref.
PVA	98000	0.0357	3.2993	302.2	2227/2227	0.025107	2808.15	[32]
ethanol	46.069	0.05172	3.1771	198.237	1/1	0.03238	2653.24	[19]
H_2O	18.015	0.06687	$\sigma(T)^b$	353.9449	1/1	0.04509	2425.67	[21]

Note: a: Segment number (m) depends on the molecular mass (M) of a polymer and it is determined from the product of m^{seg}/M (second column) and M (first column).

b: $\sigma(T) = 2.7927 + 10.11 \times e^{\left(-\frac{0.01775 * T}{K}\right)} - 1.417 \times e^{\left(-\frac{0.01146 * T}{K}\right)}$

For binary mixtures, mixture parameters such as the segment diameter (σ_{ij}) and the dispersion energy (??$_{ij}$/k) can be calculated by Berthelot-Lorentz combining rules using the pure-component PC-SAFT parameters:

$$\sigma_{ij} = \frac{1}{2}(\sigma_i + \sigma_j) \quad (2)$$

$$\varepsilon_{ij} = \sqrt{\varepsilon_i \varepsilon_j}(1 - k_{ij}) \quad (3)$$

where k_{ij} is the binary interaction parameter and is introduced to correct the segment-segment interactions of unlike chains [29].

Phase equilibrium criteria (Eq. 4) are applied to calculate the composition of the water/ethanol/PVA mixture:

$$\mu^{liq}_i(T,p,x^{liq}_i) = \mu^{pol}_i(T,p,x^{pol}_i) \tag{4}$$

where μ^{liq}_i and μ^{pol}_i are the chemical potential of component i (i.e. water or ethanol) in the liquid and polymer phase, respectively. x^{liq}_i and x^{pol}_i are the molar fraction of component i in the liquid and polymer phase, respectively.

The molar fraction of water and ethanol in the PVA membranes was determined numerically, using MATLAB 2014 to minimize the objective function [29].

$$Min = \sum_{j=1}^{N^{exp}}\left(\frac{C^{exp}_j - C^{calc}_j}{C^{exp}_j}\right)^2 \tag{5}$$

where C^{exp}_j and C^{calc}_j are the total sorbed concentrations of ethanol and water within the membrane (g/g) determined experimentally and calculated from Eq. 4, and N^{exp} is the number of experimental data points. For binary mixtures (pure ethanol or pure water in PVA), only one binary interaction parameter (k_{ij}) was used as the fitting parameter and this was determined by pure liquid sorption data at each test temperature. For ternary mixtures, an extra interaction parameter accounting for water/ethanol interaction was used with this determined from the binary mixture data to fit the sorption data provided in Fig. 2.

The pervaporation performance of the membrane was tested using a customed rig, as shown in Fig. 1. The membrane surface area was 12.56 cm^2 and the thickness was 46.3 μm. 500 ml feed solutions with 90, 85 and 80 wt% ethanol were used and a stirrer was utilized to minimize concentration polarization [33]. The operational temperature was controlled by an oven. The permeate side was maintained under vacuum and permeate vapours were collected in a cold trap immersed in liquid N_2. The membrane was kept in contact with the liquid feed at 40 °C overnight prior to measuring the permeability for each feed concentration. For each temperature, the permeate stream was collected over an interval of 0.5-2 hours and this measurement was repeated in triplicate. The permeate composition was then analyzed by a gas chromatography as described above.

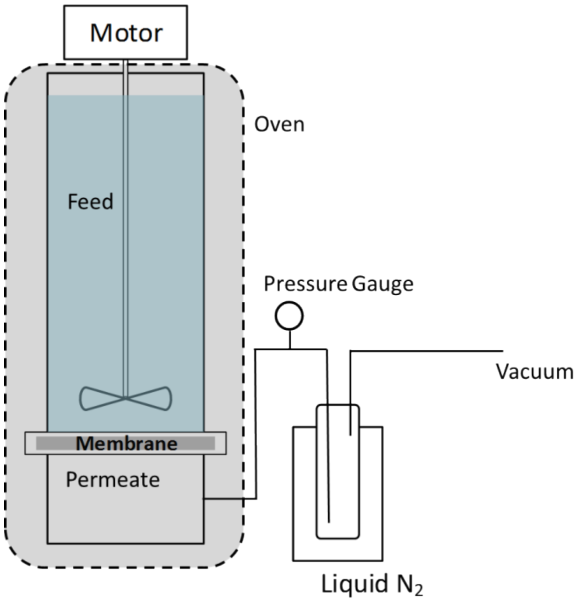

Fig. 1: Schematic diagram of the pervaporation set-up

The permeate flux *J* was determined by Eq. (6):

$$J = \frac{\Delta m}{A \Delta t} \quad (6)$$

where Δ*m*, *A* and *t* are the permeate mass, membrane area and operating time, respectively.

The separation factor (*SF*) was calculated by Eq. (7):

$$SF = \frac{y_1/y_2}{x_1/x_2} \quad (7)$$

where subscripts 1 and 2 are water and ethanol, *x* and *y* are the weight fraction of the components in the feed and permeate sides.

The permeance (P_i) of water and ethanol and selectivity (α) are further calculated by Eq. (8) and (9):

$$P_i = \frac{J_i}{x_{n,i}\gamma_i p_i^{sat} - y_{n,i} p_i^{p}} \quad (8)$$

$$\alpha = \frac{P_i}{P_j} \quad (9)$$

where Pi and J_i are the membrane permeance and flux of component i, $x_{n,i}$ and $y_{n,i}$ are the molar fractions on the feed and permeate sides. γ_i and p_i^{sat} are the activity coefficient and saturated vapour pressure of component i, which was calculated using the NRTL model in Aspen Plus V8.6. p_i^p is the permeate pressure which was set to zero.

Results and Discussion

Fig. 2 shows the total sorption of both ethanol and water into the PVA membrane at different ethanol weight concentrations as a function of temperature. For pure ethanol, the mass sorption was ~0.025g/g (PVA) across the whole experimental temperature range. However, when the ethanol concentration was lowered to 85 wt% and below, the total sorption became more dependent upon temperature. At 75 wt% ethanol concentration, for instance, total sorption increased from 0.32 at 45 °C to 0.70 g/g (PVA) at 90 °C. Similar results have been reported for PVA/APTEOS hybrid membranes [34]. It was a different case for pure water due to the inherent hydrophilicity of the membrane. The mass sorption was much higher compared with pure ethanol and it increased from 1.30 at 45 °C to 1.72 g/g (PVA) at 60 °C, then remained at around this value from 60 to 90 °C.

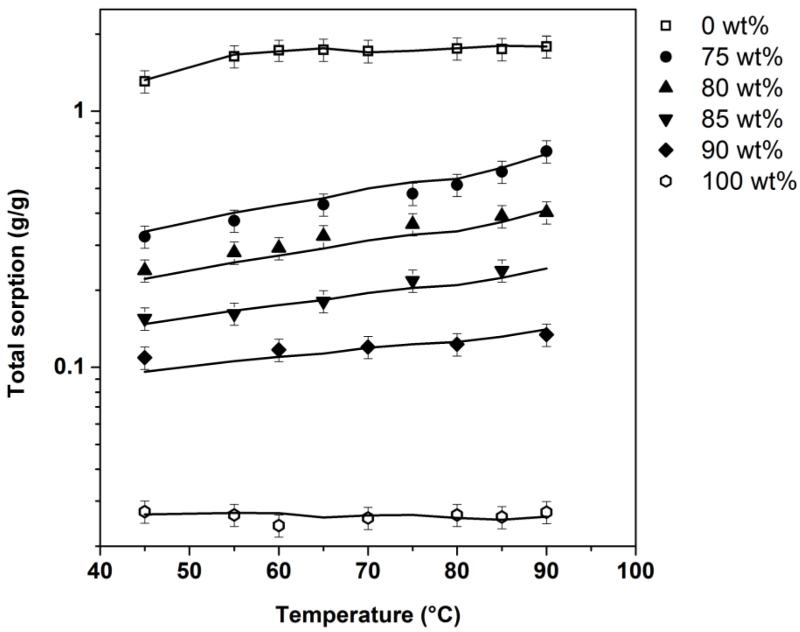

Fig. 2: Total water/ethanol sorption of the PVA membranes as a function of temperature and ethanol feed concentration (wt%). The lines are fitting results from the PC-SAFT model.

To further analyze the sorption behavior of the membrane, the PC-SAFT equation of state was applied to model this sorption data (Fig. 2). Only three interaction parameters were used in the model for this ternary mixture and all followed linear relationships with temperature with $R^2>0.994$ (see Table 2). It is clear that the predictions of the PC-SAFT model agree well with experimental data.

To further verify the model, the composition of the sorbed mixture within very thick membranes was estimated at 45 ^oC. These experiments indicated the water concentrations in the desorbed vapors at 75 wt%, 80 wt% and 85 wt% ethanol feed concentrations were 74 wt%, 69 wt% and 66 wt%, respectively. This data is consistent with model predictions of 69 wt%, 65 wt% and 61 wt%.

Although the PC-SAFT model is an equation of state, which is only valid for equilibrium systems, it provided excellent results for glassy PVA, which is in a non-equilibrium state. We have observed similar results when modelling water sorption into other glassy polymers [35] and is because the excess free volume in such polymers plays an insignificant role in the sorption process. Indeed, a type III sorption isotherm was reported for water sorption in PVA, confirming that there was little water sorption in the excess free volume [36]. Another explanation is that there may be a transition from a glassy to rubbery state as sorption occurs. This is very likely to happen in our case as the amount of sorption is high.

Table 2: Binary Interaction Parameters (k_{ij}) determined from PC-SAFT modelling of the total sorption uptake of water and ethanol into PVA, as a function of temperature (t, °C).

PVA/H_2O	PVA/ethanol	H_2O/ethanol
0.00124*t-0.11244	0.000465*t-0.01999	0.000242*t-0.03635

Using this approach, it is possible to separate the mass sorption of both water and ethanol in the PVA membrane. The heat of sorption (ΔH) of each component in the memrbane can also be readily calculated from Eq. (10):

$$S \equiv \frac{C}{P} = S_0 e^{-\Delta H / RT} \tag{10}$$

where S is solubility; C is sorption concentration; P is sorption pressure; S_0 is pre-expoential factor; R is ideal gas constant and T is sorption temperature.

Fig. 3 reports the Arrhenius plot of water and ethanol solubility in PVA membranes as a function of temperature. The solubility of both water and ethanol decreases with temperature. Both water and ethanol solubility increased with increasing water content in the feed solution as the water swelled the polymer causing an increase in free volume and chain flexbility. The calculated heat of sorption was -37 and -42 kJ mol^{-1} for pure water and ethanol which is very close to the corresponding heat of vaporisation (i.e. 40.6 kJ mol^{-1} for water and 38.6 kJ mol^{-1} for ethanol) [16,24] (see Table 3). Furher investigation is needed to confirm the state of both penetrants in the membrane.

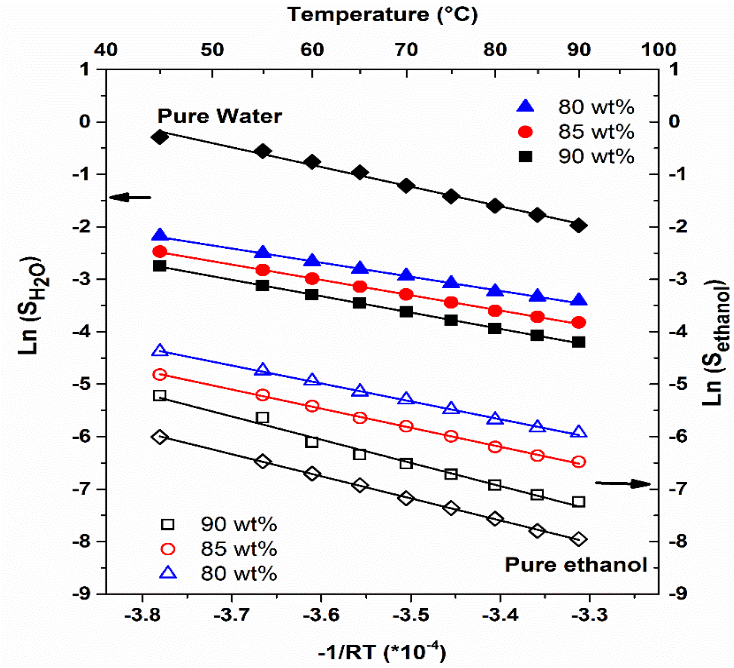

Fig. 3: Arrhenius plot of water and ethanol solubility in PVA (lines: fitting results).

The influence of operational temperature and feed compositions on membrane performance was carefully investigated and the results are shown in Fig. 4. In general, the water flux increased when operational temperature increased, while the separation factor displayed an opposite trend. The ideal selectivity showed a similar trend to the separation factor (data not shown). These trends are expected as the driving force (i.e. vapor pressure) is an exponential function of temperature. Moreover, the fractional free volume of the polymer matrix increases when temperature increases, resulting in an increase of the diffusivities of penetrants. At 90 wt% ethanol feed concentration, water flux increased from 47 g m^{-2} h^{-1} at 60 °C to 191 g m^{-2} h^{-1} at

95 °C while the separation factor decreased from 103 to 35, indicating the influence of temperature on ethanol flux was more significant than on the water flux. When the ethanol feed concentration was dropped to 85 wt%, there was a significant increase in the water flux compared with 90 wt% ethanol feed concentration.

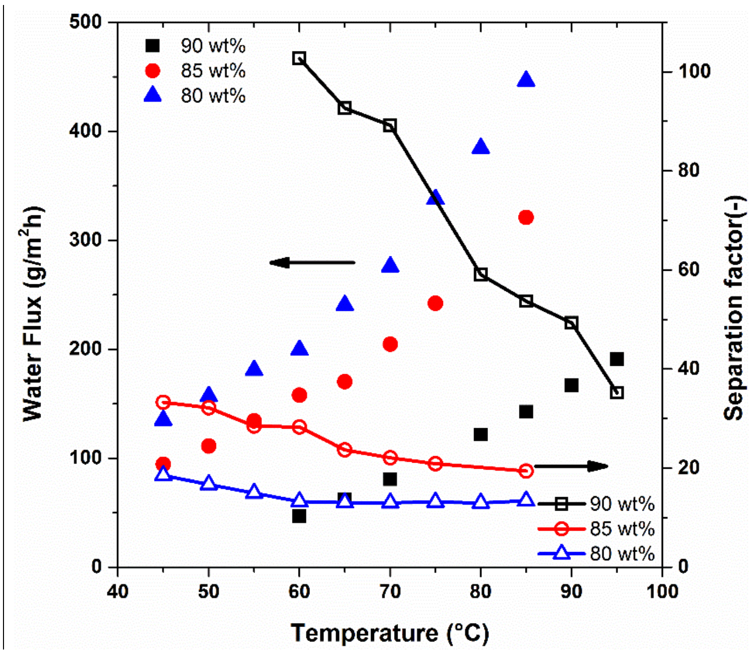

Fig 4: Pervaporation performance of the PVA membrane as a function of operational temperature and feed concentration. Note: lines are provided as a guide only.

The water flux and separation factor is widely reported to represent pervaporation performance [3,4,37] but there is significant variation in the reported literature data. For example, a PVA membrane using glutaraldehyde as a cross-linker showed a flux of 50 g m^{-2} h^{-1} and separation factor of 180 at 90 wt% ethanol feed concentration at 30 °C for ethanol dehydration [20]. On the other hand, a commercial PERVAP 2510 membrane had a flux of 2456 g m^{-2} h^{-1} and separation factor of 15 at 80 wt% ethanol feed concentration at 80 °C [38]. Indeed, these changes arise not only from the intrinsic properties of the membrane but are affected by operational conditions such as feed composition, operational temperature and permeate pressure [39] and membrane thickness. To better investigate membrane properties, the water and ethanol permeance values were calculated according to Eq. (4) (Fig. 5). When reported on this basis, some surprising trends emerge in the water permeance data. It is clear that there is a transition temperature range for each feed concentration, with different transport behavior occurring on either side of this transition. This transition temperature decreased from 70-80 °C to 60-65 °C when the ethanol feed concentration decreased from 90 to 80 wt%. It is hypothesized that these temperatures correspond to a glass transition occurring due to sorption of the water/ethanol mixture, resulting in a change of transport behavior. The pristine PVA membrane has a glass transition temperature (T_g) of 95-100 °C, supported by differential scanning calorimetry (data not shown) and it is expected that this transition temperature would decrease upon penetrant addition [27]. As the membrane is hydrophilic, the magnitude of this decline would be expected to be greater at 80 wt% feed ethanol concentration than that at 90 wt% due to the greater water uptake. On the other hand, there was only a transition observed at 80 wt% feed concentration for ethanol, with no obvious change in the permeance gradient at 90 and 85 wt%.

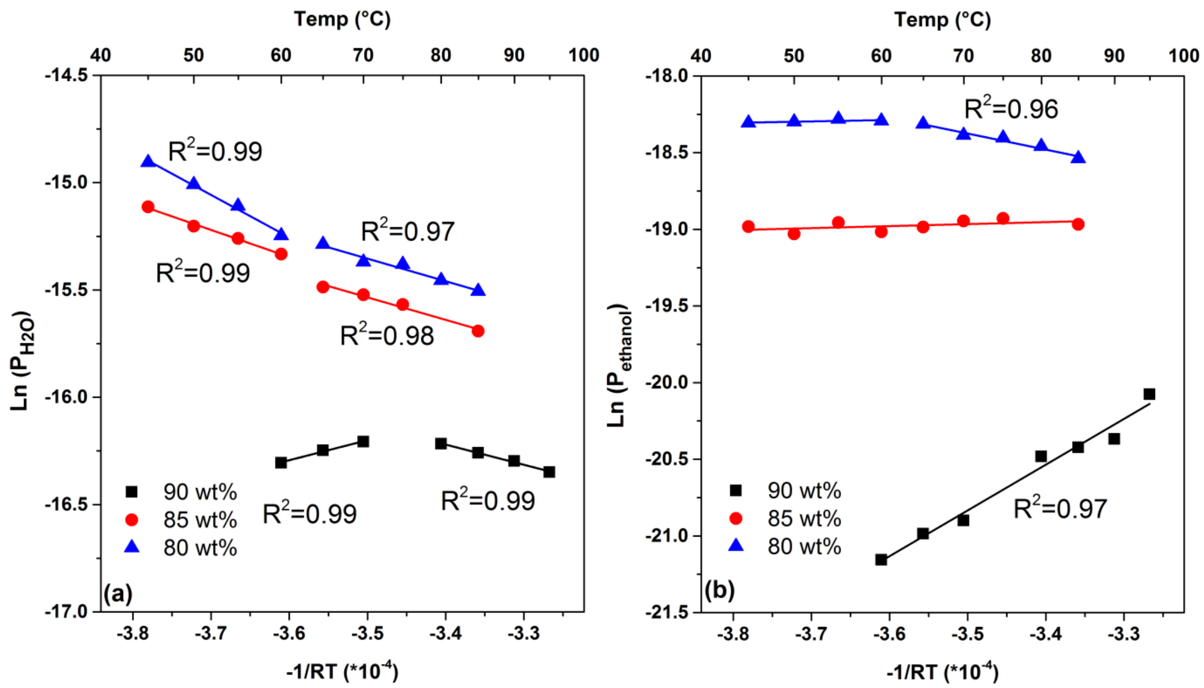

Fig. 5: Arrhenius plot of water (a) and ethanol permeance (b) as a function of feed ethanol concentration (lines are a linear regression). The experimental error of permeance was within ±5%.

The apparent activation energy is a combined effect of the heat of sorption (ΔH) and the energy of diffusion (E_d), and $E_a=\Delta H+E_d$. A positive E_a indicates that diffusion is dominant in the transport process and a negative E_a means that the transport is governed by sorption.

The E_a of water changed from 9.3 to -9.4 kJ mol^{-1} at 90 wt% after glass transition, suggesting a transition from diffusion controlled transport to sorption controlled transport. When the temperature was below 70 °C, the degree of swelling was small (due to the high concentration of ethanol) and hence the membrane was in a glassy state. Under these circumstances, diffusion was the limiting factor, evidenced by an E_d of 41 kJ mol^{-1} , Similar results have been reported for a PVA membrane using citric acid as cross-linker [16]. When the temperature was above 80 °C, the E_d was reduced to 22 kJ mol^{-1}. This reduction may not be simply explained by a glassy to rubbery transition, which should lead to an increase of $E_{d,}$ as evidenced by both experimental and theoretical work [40]. It is also unlikely to relate to a change in crystallinity, as this should reduce at higher temperatures, again leading to an increase of E_d.

An alternative assessment might be made based on our prior work with a comparable hydrophilic polymer, Sulphonated Poly(Ether Ether)Ketone (SPEEK) [25]. We observed that the activation energy for diffusion changed from a positive value at low temperatures to a negative one at higher temperatures. We speculated that the falling diffusion coefficient with increasing temperature related to an increase in the total water concentration within the membrane at higher temperatures due to the higher saturation partial pressure of water. This reduction in diffusion coefficient with increasing penetrant concentration is known as 'antiplasticisation'. It is commonly attributed to solvent molecules accumulating in the larger free volume voids and reducing the total free volume available for diffusion [41–45]. However in the present case, at 90 wt% ethanol, the total sorbed concentration is at its lowest (see Fig. 2) so antiplasticisation through clustering of water and/or ethanol molecules would appear unlikely.

Alternatively, the behavior may relate to the relationship between 'bound' or 'non-freezing' water; and 'bound' ethanol molecules which are hydrogen bonded to the PVA polymer. Such bound molecules are less mobile and thus have lower diffusion coefficients [46]. However, bound water has also been shown to contribute most strongly to the plasticisation of the polymer by disrupting polymer to polymer hydrogen bonds [47]. Free volume models of plasticization and antiplasticisation do not take such strong polymer/solvent interactions into account [40]. For 90 wt% ethanol, it is possible that there is a loss of bound water at higher temperatures, which allows more polymer-polymer bonding to occur, and thus increases in free volume with temperature to be smaller.

At 85 wt% feed concentration, the E_a was -12.8 kJ mol^{-1} before glass transition occurred, indicating a sorption-controlled transport behavior. The membrane had a higher degree of swelling when the water concentration increased (Fig. 2). It is worthwhile noting that the influence of penetrant concentration in the membrane also played a vital role in the transport behavior. It is known that a penetrant dissolved in the polymer can swell the polymer matrix.

A higher degree of swelling can also result in an increase of chain mobility even though the polymer is in a glassy state. Hence, the penetrant can pass through the polymer matrix easier and lower energy is needed (i.e. a reduction of E_d). Indeed, the E_a was further decreased to -20.2 kJ mol^{-1} at 80 wt% feed concentration when the membrane was in a glassy state. It is interesting that the E_a was -10.5 kJ mol^{-1} when the membrane was in rubbery state. Considering the heat of sorption was constant (Fig. 3), the increase of E_a suggests that there was an increase of E_d after glass transition occurred.

The E_a of ethanol was 29.9 kJ mol^{-1} at 90 wt% ethanol feed concentration across the full range of temperatures. Ethanol has a much larger kinetic diameter (4.5 Å) than water (2.65 Å) [48]; hence, a much higher E_d is needed for ethanol to permeate through the membrane. This E_d was significantly reduced at 85 wt% feed concentration due to the increased membrane swelling. At 80 wt% ethanol feed concentration, a transition was again observed when the temperature was higher than 65 °C. There appears to be a decline in E_d after the glass transition, which is similar to that of water at 90 wt%. Again, it is possible that this relates to changes in the hydrogen boning or clustering within the polymer as temperature and absolute concentrations change.

Table 3: Activation energy of water and ethanol in the membrane at different ethanol feed concentrations.

For transport of water molecules:

	90 wt% ethanol		85 wt% ethanol		80 wt% ethanol	
ΔH_s (kJ mol^{-1})	-31		-29		-27	
Transition temperature (T_t)	70-80 °C		60-65 °C		60-65 °C	
	< 70 °C	> 80 °C	<60 °C	>65 °C	<60 °C	>65 °C
E_a (kJ mol^{-1})	9.6	-9.1	-12.8	-10.5	-20.2	-10.9
E_d (kJ mol^{-1})	41	22	16	19	7	16

For transport of ethanol molecules:

	90 wt% ethanol	85 wt% ethanol	80 wt% ethanol	
ΔH_s (kJ mol^{-1})	-44	-36	-34	
Transition temperature (T_t)	-	-	60-65 °C	
			<60 °C	>65 °C
E_a (kJ mol^{-1})	29.9	1.6	1.4	-10
E_d (kJ mol^{-1})	74	38	35	24

To separate the contribution of solubility and diffusivity to the total membrane selectivity, sorption selectivity (α_s) and diffusion selectivity (α_d) is calculated using the results from PC-SAFT model (Fig. 3) and the data is shown in Fig. 6. The sorption selectivity α_s slightly increased when temperature increased for all three feed concentrations and was higher at 90 wt% feed concentration than at 80 wt%. On the other hand, diffusion selectivity (α_d) decreased as temperature increased. Specifically, it decreased from 7.7 at 60 °C to 2.83 at 90 °C at 90 wt% ethanol. This is because the ethanol diffusion coefficient changes more dramatically with temperature (Fig. 5 and Table 3) due to its larger kinetic diameter. At 80 wt% ethanol concentration, α_d was in the range of 1.7-3.3, which was much lower than that at 90 wt% at all temperatures. This reduction may be attributed to the high degree of swelling of the membrane (Fig. 2), resulting in a more flexible chain structure.

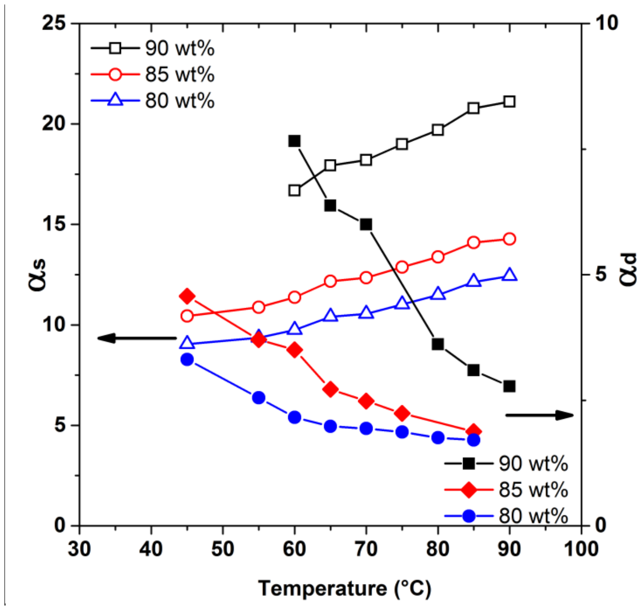

Fig. 6: Sorption (α_s) and diffusion (α_d) selectivity of water over ethanol for the PVA membrane. Note: lines are provided as a guide only.

Conclusions

Crosslinked PVA membranes were prepared using glutaraldehyde as a cross-linker. The sorption of water/ethanol mixture in the membrane was affected by both solution composition and sorption temperature. The mixture sorption data was successfully modeled by PC-SAFT model and the sorption of each component was determined individually. The solubility of both water and ethanol decreased with temperature, and the influence of feed concentration was marginal.

The pervaporation data of the membrane was then analyzed in terms of permeance and ideal selectivity. Different from water flux, water permeance decreased when temperature increased. A significant increase in water permeance was observed when the ethanol feed concentration decreased from 90 to 80 wt%. Apparent activation energy analysis revealed more information about the transport of water and ethanol through the membrane. For water, there was a transition in the operational temperature range across which different E_a were observed. The E_a changed from 9.6 to -9.1 kJ mol^{-1} at 90 wt% feed concentration due to the influence of the glass transition, but in a manner that was not consistent with the usual increase in diffusion coefficient that occurs when a polymer becomes rubbery. For ethanol, the E_a was 29.9 kJ mol^{-1} at 90 wt% feed concentration, indicating that the mass transport was controlled by diffusion. It decreased from 1.4 to -10 kJ mol^{-1} at 80 wt% feed concentration, again in a manner not commonly observed for a glassy to rubbery transition. The sorption selectivity of the membrane increased when the ethanol feed concentration increased and the diffusion selectivity also achieved a higher value at high ethanol feed concentration (i.e. 90 wt%).

Acknowledgements

The authors acknowledge funding support from the Australian Research Council (ARC) Discovery Program (DP150100977).

References

[1] P. Shao, R.Y.M. Huang, Polymeric membrane pervaporation, J. Memb. Sci. 287 (2007) 162–179.

[2] P.D. Chapman, T. Oliveira, A.G. Livingston, K. Li, Membranes for the dehydration of solvents by pervaporation, J. Memb. Sci. 318 (2008) 5–37.

[3] M. Amirilargani, B. Sadatnia, Poly (vinyl alcohol)/ zeolitic imidazolate frameworks (ZIF-8) mixed matrix membranes for pervaporation dehydration of isopropanol, J. Memb. Sci. 469 (2014) 1–10.

[4] X. Feng, R.Y.M. Huang, Liquid Separation by Membrane Pervaporation: A Review, Ind. Eng. Chem. Res. 36 (1997) 1048–1066.

[5] J. Wijmans, R. Baker, The solution-diffusion model: a review, J. Memb. Sci. (1995).

[6] D. Hua, Y.K. Ong, Y. Wang, T. Yang, T.-S. Chung, ZIF-90/P84 mixed matrix membranes for pervaporation dehydration of isopropanol, J. Memb. Sci. 453 (2014) 155–167.

[7] T. Gallego-Lizon, E. Edwards, G. Lobiundo, L. Freitas dos Santos, Dehydration of water/t-butanol mixtures by pervaporation: comparative study of commercially available polymeric, microporous silica and zeolite membranes, J. Memb. Sci. 197 (2002) 309–319.

[8] D.W. Mangindaan, G. Min Shi, T.-S. Chung, Pervaporation dehydration of acetone using P84 co-polyimide flat sheet membranes modified by vapor phase crosslinking, J. Memb. Sci. 458 (2014) 76–85.

[9] M. Peng, L. Vane, S. Liu, Recent advances in VOCs removal from water by pervaporation, J. Hazard. Mater. (2003).

[10] B. Smitha, D. Suhanya, S. Sridhar, Separation of organic–organic mixtures by pervaporation—a review, J. Membr. (2004).

[11] K.-R. Lee, J.-Y. Lai, Pervaporation of aqueous alcohol mixtures through a membrane prepared by grafting of polar monomer onto nylon 4, J. Appl. Polym. Sci. 57 (1995) 961–968.

[12] X.-S. Wang, Q.-F. An, Q. Zhao, K.-R. Lee, J.-W. Qian, C.-J. Gao, Homogenous polyelectrolyte complex membranes incorporated with strong ion-pairs with high pervaporation performance for dehydration of ethanol, J. Memb. Sci. 435 (2013) 71–79.

[13] V.S. Praptowidodo, Influence of swelling on water transport through PVA-based membrane, J. Mol. Struct. 739 (2005) 207–212.

[14] C.-K. Yeom, K.-H. Lee, Pervaporation separation of water-acetic acid mixtures through poly(vinyl alcohol) membranes crosslinked with glutaraldehyde, J. Memb. Sci. 109 (1996) 257–265.

[15] M.N. Hyder, R.Y.M. Huang, P. Chen, Correlation of physicochemical characteristics with pervaporation performance of poly(vinyl alcohol) membranes, J. Memb. Sci. 283 (2006) 281–290.

[16] M.C. Burshe, S.B. Sawant, J.B. Joshi, V.G. Pangarkar, Sorption and permeation of binary water-alcohol systems through PVA membranes crosslinked with multifunctional crosslinking agents, Sep. Purif. Technol. 12 (1997) 145–156.

[17] H. Feng, Modeling of vapor sorption in glassy polymers using a new dual mode sorption model based on multilayer sorption theory, Polymer. 48 (2007) 2988–3002.

[18] T.-H. Yang, S. Jessie Lue, UNIQUAC and UNIQUAC-HB models for the sorption behavior of ethanol/water mixtures in a cross-linked polydimethylsiloxane membrane, J. Memb. Sci. 415 (2012) 534–545.

[19] J. Gross, G. Sadowski, Application of the Perturbed-Chain SAFT Equation of State to Associating Systems, Ind. Eng. Chem. Res. 41 (2002) 5510–5515.

[20] L. Hesse, S. Naeem, G. Sadowski, VOC sorption in glassy polyimides-Measurements and modeling, J. Memb. Sci. 415–416 (2012) 596–607.

[21] M.C. Arndt, G. Sadowski, Modeling Poly(*N* -isopropylacrylamide) Hydrogels in Water/Alcohol Mixtures with PC-SAFT, Macromolecules. 45 (2012) 6686–6696.

[22] L. Hesse, G. Sadowski, Modeling Liquid–Liquid Equilibria of Polyimide Solutions, Ind. Eng. Chem. Res. 51 (2012) 539–546.

[23] C.K. Yeom, S.H. Lee, J.M. Lee, Pervaporative permeations of homologous series of alcohol aqueous mixtures through a hydrophilic membrane, J. Appl. Polym. Sci. 79 (2001) 703–713.

[24] X. Feng, R.Y.M. Huang, Estimation of activation energy for permeation in pervaporation processes, J. Memb. Sci. 118 (1996) 127–131.

[25] H. Azher, C. Scholes, S. Kanehashi, G. Stevens, S. Kentish, The effect of temperature on the permeation properties of Sulphonated Poly (Ether Ether) Ketone in wet flue gas streams, J. Memb. Sci. 519 (2016) 55–63.

[26] H. Sijbesma, K. Nymeijer, R. van Marwijk, R. Heijboer, J. Potreck, M. Wessling, Flue gas dehydration using polymer membranes, J. Memb. Sci. 313 (2008) 263–276.

[27] J. Potreck, F. Uyar, H. Sijbesma, K. Nijmeijer, D. Stamatialis, M. Wessling, Sorption

induced relaxations during water diffusion in S-PEEK, Phys. Chem. Chem. Phys. 11 (2009) 298–308.

[28] S. Sato, M. Suzuki, S. Kanehashi, K. Nagai, Permeability, diffusivity, and solubility of benzene vapor and water vapor in high free volume silicon- or fluorine-containing polymer membranes, J. Memb. Sci. 360 (2010) 352–362.

[29] J. Gross, G. Sadowski, Perturbed-Chain SAFT: An Equation of State Based on a Perturbation Theory for Chain Molecules, Ind. Eng. Chem. Res. 40 (2001) 1244–1260.

[30] M. Kleiner, G. Sadowski, Modeling vapor–liquid equilibria of ethanol+1,1,1,2,3,3,3-heptafluoropropane binary mixtures using PC-SAFT, Fluid Phase Equilib. 260 (2007) 190–194.

[31] F. Tumakaka, J. Gross, G. Sadowski, Thermodynamic modeling of complex systems using PC-SAFT, Fluid Phase Equilib. 228–229 (2005) 89–98.

[32] H.-S. Byun, B.-S. Lee, Liquid-liquid equilibrium of hydrogen bonding polymer solutions, Polymer. 121 (2017) 1–8.

[33] H. Azher, C.A. Scholes, G.W. Stevens, S.E. Kentish, Water permeation and sorption properties of Nafion 115 at elevated temperatures, J. Memb. Sci. 459 (2014) 104–113.

[34] Q.G. Zhang, Q.L. Liu, Z.Y. Jiang, Y. Chen, Anti-trade-off in dehydration of ethanol by novel PVA/APTEOS hybrid membranes, J. Memb. Sci. 287 (2007) 237–245.

[35] L. Liu, S.E. Kentish, Modeling of carbon dioxide and water sorption in glassy polymers through PC-SAFT and NET PC-SAFT, Polymer. 104 (2016) 149–155.

[36] E.E. Shafee, H.. Naguib, Water sorption in cross-linked poly(vinyl alcohol) networks, Polymer. 44 (2003) 1647–1653.

[37] T.A. Peters, N.E. Benes, J.T.F. Keurentjes, Hybrid ceramic-supported thin PVA pervaporation membranes: Long-term performance and thermal stability in the dehydration of alcohols, J. Memb. Sci. 311 (2008) 7–11.

[38] Z. Huang, H.M. Guan, W.L. Tan, X.Y. Qiao, S. Kulprathipanja, Pervaporation study of aqueous ethanol solution through zeolite-incorporated multilayer poly(vinyl alcohol) membranes: Effect of zeolites, J. Memb. Sci. 276 (2006) 260–271.

[39] R.W. Baker, J.G. Wijmans, Y. Huang, Permeability, permeance and selectivity: A preferred way of reporting pervaporation performance data, J. Memb. Sci. 348 (2010) 346–352.

[40] J.S. Vrentas, C.M. Vrentas, Solvent Self-Diffusion in Glassy Polymer-Solvent Systems, Macromolecules. 27 (1994) 5570–5576.

[41] Y. Maeda, D.R. Paul, Effect of antiplasticization on gas sorption and transport. III. Free volume interpretation, J. Polym. Sci. Part B Polym. Phys. 25 (1987) 1005–1016.

[42] J.S. Lee, W. Madden, W.J. Koros, Antiplasticization and plasticization of Matrimid® asymmetric hollow fiber membranes. Part B. Modeling, J. Memb. Sci. 350 (2010) 242–251.

[43] Q. Liu, M. Galizia, K.L. Gleason, C.A. Scholes, D.R. Paul, B.D. Freeman, Influence of toluene on CO2 and CH4 gas transport properties in thermally rearranged (TR) polymers based on 3,3′-dihydroxy-4,4′-diamino-biphenyl (HAB) and 2,2′-bis-(3,4-dicarboxyphenyl) hexafluoropropane dianhydride (6FDA), J. Memb. Sci. 514 (2016) 282–293.

[44] G.Q. Chen, C.A. Scholes, C.M. Doherty, A.J. Hill, G.G. Qiao, S.E. Kentish, Modeling of the sorption and transport properties of water vapor in polyimide membranes, J. Memb. Sci. 409–410 (2012) 96–104.

[45] G.Q. Chen, S. Kanehashi, C.M. Doherty, A.J. Hill, S.E. Kentish, Water vapor permeation through cellulose acetate membranes and its impact upon membrane separation performance for natural gas purification, J. Memb. Sci. 487 (2015) 249–255.

[46] C. Wu, Cooperative behavior of poly(vinyl alcohol) and water as revealed by molecular dynamics simulations, Polymer. 51 (2010) 4452–4460.

[47] R.M. Hodge, T.J. Bastow, G.H. Edward, G.P. Simon, A.J. Hill, Free Volume and the Mechanism of Plasticization in Water-Swollen Poly(vinyl alcohol), Macromolecules. 29 (1996) 8137–8143.

[48] T. Borjigin, F. Sun, J. Zhang, K. Cai, H. Ren, G. Zhu, M.S. Lah, M. O'Keeffe, O.M. Yaghi, C. Kreuz, J.S. Chang, Y.K. Hwang, V. Marsaud, P.N. Bories, L. Cynober, S. Gil, G. Ferey, P. Couvreur, R. Gref, A microporous metal–organic framework with high stability for GC separation of alcohols from water, Chem. Commun. 48 (2012) 7613.